Int. J. Heat Mass Transfer. Vol. 20, pp. 1389–1399. Pergamon Press 1977. Printed in Great Britain

DYNAMIC INSTABILITIES IN TUBES OF A LARGE CAPACITY, STRAIGHT-TUBE, ONCE-THROUGH SODIUM HEATED STEAM GENERATOR

H. C. ÜNAL, M. L. G. VAN GASSELT
TNO, P.O. Box 342, Apeldoorn, The Netherlands

and

P. W. P. H. LUDWIG
NERATOOM, P.O. Box 2244, The Hague, The Netherlands

(*Received* 10 *January* 1977)

Abstract—Density-wave type dynamic instabilities were detected in the tubes of a large-capacity sodium heated steam generator. The peak-to-peak amplitudes of these oscillations varied between 9 and 60 K and the periods between 4 and 7.6 s.

Our experimental data for the periods and the inception conditions of the dynamic instabilities, and the data found in literature obtained for a tube and a rectangular channel across which pressure drop is constant, have been correlated with simple equations for the following range of conditions: pressure: 4.1–17 MN/m^2; exit quality: 0.27–1.59; inlet subcooling: 3–111 K; ratio of heated length to hydraulic diameter: 153–1921; hydraulic diameter: 0.0045–0.0126 m; enthalpy rise in the channel: 582–2130 kJ/kg; mass velocity: 353–2088 kg/m^2 s; average heat flux 0.1–3.25 MW/m^2; period: 0.35–7.6 s.

At the start of dynamic instabilities the steam quality (or the enthalpy of the steam or steam/water mixture) at the outlet of a boiling channel is constant for a given subcooling, pressure and geometry in the low-subcooling range, and for a given pressure and geometry for the range of medium and high subcoolings.

The period of the dynamic instabilities is a function of the transit time of a fluid particle in the boiling region of a channel, the Froude number and the ratio of the length of the boiling region to the total heated length.

A hot channel factor has also been established, which relates the operating conditions in the tube in which the dynamic instabilities occur first, to the average operating conditions in the steam generator.

NOMENCLATURE

A_F, cross-sectional area [m^2];
A_H, heated area [m^2];
D, inside diameter of a tube [m];
D_H, hydraulic diameter [m];
Fr, Froude number ($Fr = G^2/\rho_s^2 D_H g$);
G, mass velocity [kg/m^2 s];
g, acceleration of gravity [m/s^2];
H, enthalpy [J/kg];
ΔH, enthalpy rise in a channel [J/kg];
ΔH_{sub}, inlet sub cooling in units of enthalpy [J/kg];
K, pressure loss coefficient of an orifice or a flow control valve fitted to the inlet of a channel, based on the flow area of the channel;
L, heated length or a length [m];
P, pressure [N/m^2];
P_c, critical pressure [N/m^2];
P_r, reduced pressure ($P_r = P/P_c$);
Q, power [W];
q, heat flux [W/m^2];
Re, Reynolds number ($Re = GD_H/\nu_l$);
r, latent heat of evaporation [J/kg];
t, temperature [K or °C];
Δt_{sub}, degree of subcooling [K];
Δt_l, logarithmic mean temperature difference [K];
U, over-all coefficient of heat transfer [W/m^2 K];
W, mass flow [kg/s];
X, steam quality;
z, axial coordinate [m].

Greek symbols

α, void fraction;
β, vapour volumetric rate ratio;
ν, viscosity [kg/m s];
ρ, density [kg/m^3];
ξ, transit time of a fluid particle [s];
ζ, period [s].

Subscripts

a, refers to average value;
b, refers to boiling region;
I, refers to inception conditions of dynamic instabilities;
i, refers to inlet condition;
p, refers to preheat region;
o, refers to outlet condition;
S, refers to superheated steam region;

s, refers to saturated liquid condition;
sg, refers to unit or steam generator;
v, refers to saturated vapour condition.

INTRODUCTION

DYNAMIC instabilities are hazardous for a sodium heated steam generator, which is a crucial component of a LMFBR, since they induce flow maldistribution among the tubes or in the tubes, and thermal cyclings at the welds, at the upper tube plate and at the dry-out location.

Very little literature exists on experimental and theoretical works dealing with the dynamic instabilities in a tube of a long, straight-tube, once-through, sodium heated steam generator [1–3]. In connection with the development of BWRs and PWRs, this type of instability has been extensively studied for short, electrically heated channels. The data from electrically heated channels can, by no means, be extrapolated to a long, sodium heated steam generator tube without any experimental verification, owing to intolerable errors in predicting the Inception Conditions of dynamic Instabilities (ICI) (i.e. power, subcooling, mass velocity and pressure at the start of instabilities) for a wide range of conditions with the existing stability models, as demonstrated in [4, 5]. There is equally little literature on stability models that can be applied to a sodium heated steam generator tube, in which superheated steam is produced [2, 3]. It is moreover reported in [6] that the model given in [3] does not fit the data sufficiently well.

The aim of this paper is to present data and correlations for the periods and the inception conditions of dynamic instabilities obtained in the tubes of a large capacity sodium heated steam generator. Before presentation of the data, dynamic instabilities relevant to a steam generator tube are briefly reviewed below. For a more detailed review of the literature on the subject, the reader is referred to [7, 8].

Many types of dynamic instabilities can occur in a steam generator tube, which can be ascribed to a number of different causes, viz. propagation of pressure- or density waves [7], variation of flow patterns [9] and thermodynamic non-equilibrium between the phases in the superheated steam region [1, 10]. However, sufficient evidence has been given in the literature that the cause of the main type of instability important for the design of steam generators is the propagation of density waves. This type of low-frequency instability is referred to in the literature as parallel-channel [3], density-wave [11], time-delay [12] or mass flow-void feed-back [4] instability or oscillations.

Density-Wave Oscillations (DWO) have been experimentally studied by many investigators for different types of geometries and boundary conditions, for water [1, 13–17] and refrigerants [11, 18], for forced- [1, 11, 13, 18] and natural-circulation systems [14–17], for a single channel [1, 13] or multi-channels [18] across which a constant pressure drop is maintained, and for a forced-convection channel to which a compressible volume such as a surge tank or a gas pressuriser is attached upstream [11]. In these investigations heat generation was either uniform [11, 13–16, 18] or non-uniform [1, 17].

The conclusions of these studies are the following:

(i) DWO are due to multiple regenerative feedbacks between flow rate, vapour generation rate and pressure drop [4, 11].

(ii) The other parameters being constant, the stability of a steam generator tube may be increased by decreasing the heat flux [1, 13], exit pressure drop [15], heated length [18] and inlet subcooling at low subcoolings [15, 16, 18], and by increasing the flow [1, 13], pressure [15, 16], inlet pressure drop [14, 15], inlet subcooling at high- and medium subcoolings [15, 16, 18] and tube diameter [16]. A non-uniform heat flux distribution stabilises the flow [17].

(iii) A coarse correlation has been found in the literature [8] indicating that the period of the DWO is approximately one to two times the transit time of a fluid particle in a tube. However, it is reported in [1, 19] that the period of the DWO can be about half or even a small fraction of the transit time.

There are some types of dynamic instabilities present always in a steam generator tube which produces superheated steam of qualities up to about 2. The temperature at any point in a cross-section in the superheated steam region of such a steam generator tube oscillates irregularly owing to thermodynamic non-equilibrium between the phases (i.e. the presence of water droplets in the superheated steam). The actual degree of superheating of the produced steam is found to be higher than that calculated by a simple heat balance, as the heat needed for the evaporation of water droplets is used for superheating [1, 10].

If an adiabatic section follows the heated section of a steam generator tube, these instabilities disappear, as observed in the present study and in [10]. This is probably due to complete evaporation of the water droplets in the highly superheated steam along the adiabatic section.

Mass-flow oscillations were also reported at the outlet of a horizontal steam generator tube [20].

TEST SET-UP, PROCEDURE AND CONDITIONS

Test set-up

Dynamic instabilities were investigated in the evaporator of a 50 MWth liquid sodium heated steam generator. This steam generator was designed by Neratoom for the LMFBR, SNR-300. It was tested in the 50 MW Sodium Component Test Facility at Hengelo. The steam generator consists of an evaporator and a superheater. A description of the steam generator is given in [21, 22]; data for the 50 MW Sodium Component Test Facility may be found in [23].

The evaporator is a counterflow, 30 MWth once-through unit and operates in forced-convection mode.

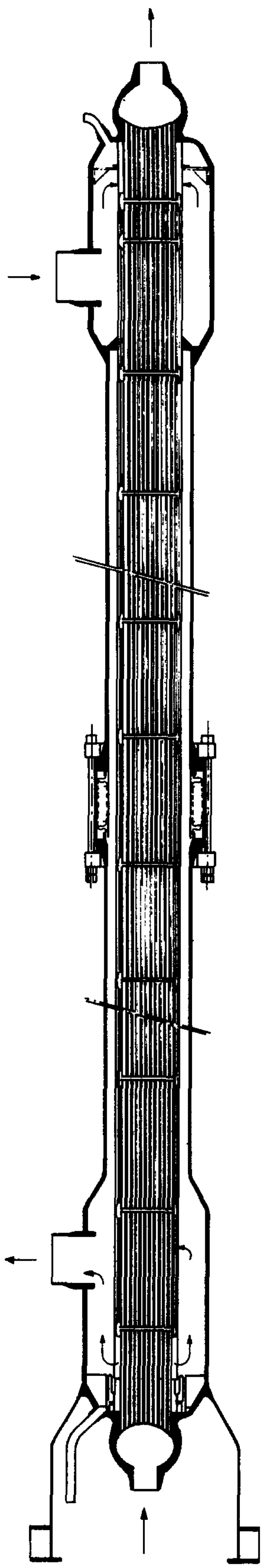

FIG. 1. Evaporator.

It is shown in Fig. 1. The water/steam flows vertically upward in 139 tubes of 0.0126 m I.D. and 0.0172 m O.D., and is heated by sodium flowing downward around the tubes arranged in a shell in an equitriangular pattern of 0.0275 m pitch. The effective (i.e. heated) tube length is 18.64 m, and the total tube length between the tube plates 19.34 m. The steam generator was manufactured from $2\frac{1}{4}$ Cr 1 Mo stabilised ferritic steel.

The evaporator was heavily instrumented [22]. It will be sufficient to mention here that the values of the inlet and outlet temperatures, outlet pressure and mass flow both at the sodium- and water/steam-side in the evaporator were measured with pre-calibrated instruments, and collected with an on-line data acquisition system and processed by a computer, Siemens-300.

In order to detect the instabilities, six thermocouples were placed on the upper tube plate at the outlets of six tubes at different radial locations, as indicated in Fig. 2. The temperatures measured by these thermocouples are recorded both with potentiometric multi-channel recorders and with the computer. In the present work, only the instabilities detected in these six tubes are dealt with; the inlet temperature and outlet pressure for these tubes are known since these quantities are equal for all the tubes in the evaporator. The pressure drop across the tubes of the evaporator is also equal for each tube.

All the temperatures were measured with inconel-sheathed, chromel–alumel thermocouples of 1 mm O.D.; the error in determining a temperature was 3/8% Water/steam-side mass flow was measured with an orifice meter with an accuracy of 2%. Sodium-side mass flow was measured with an electromagnetic flow meter with an accuracy of less than 4%. The pressures were measured with Barton cells with an accuracy of less than 2%.

Test procedure and conditions

At all operating conditions of SNR-300, the evaporator produces wet steam of qualities of 0.95 or less, and it is not susceptible to instabilities. Under extreme conditions far remote from the operating conditions of SNR-300, instabilities were observed, however, when steam with a high degree of superheating had to be produced in the evaporator; in other words the evaporator operated as a once-through steam generator for the test runs for which the instabilities have been detected, and will therefore be referred to as the unit further on.

The ICI are, per definition, the operating conditions at the last stable condition in a channel. Therefore, to determine ICI, steam quality at the outlet of the unit was increased by very small increments by decreasing water/steam-side mass flow while keeping the other operating conditions constant both at the water/steam- and sodium side. Instabilities were detected only for the aforesaid six tubes by recording the temperatures measured by the thermocouples located at the outlets of these tubes. When the first diverging temperature oscillations were detected for a tube, the

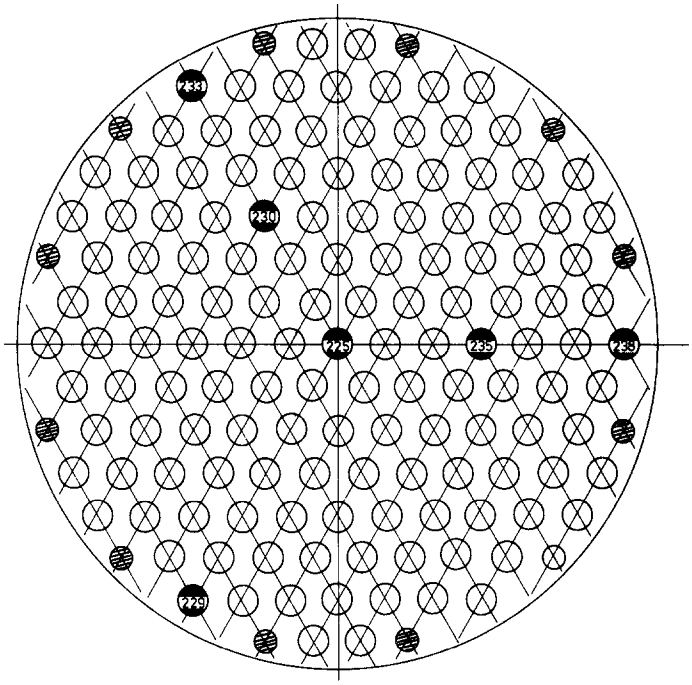

FIG. 2. Locations of the tubes for which instabilities have been detected.

Table 1. Data for the ICI and the periods of instabilities

	Location 233		Location 238		Location 229		Location 235 or 225	
Run No.	t_0 (°C)	ζ (s)	t_0 (°C)	ζ (s)	t_0 (°C)	ζ (s)	t_0 (°C)	ζ (s)
1.3*	437†	—	433†	7	—	—	—	—
2.4	428†	—	—	—	—	—	—	—
2.5	—	—	428	6.7	—	—	—	—
3.7	408†	—	405†	7.5	405†	7	—	—
4.4	399†	—	399†	6.7	—	—	—	—
13.2	430†	—	427†	5	427	5.5	—	—
13.4	—	—	—	—	—	—	430/431‡	6/6‡
14.0	418†	—	—	—	—	—	—	—
14.2	—	—	429	7.6	—	—	—	—
14.3	—	—	—	—	434	6	—	—
14.4	—	—	—	—	—	—	423‡	6.6‡
14.5	—	—	—	—	—	—	430	7.5
15.0	418†	—	—	—	—	—	—	—
15.4	—	—	431	6.6	431	7	—	—
19.7	382†	5	—	—	—	—	—	—
19.8	—	—	—	—	372	6	—	—
20.3	386†	4	—	—	—	—	—	—
21.3	367†	4	—	—	—	—	—	—
21.8	—	—	—	—	389	5	—	—
22.1	380†	4	—	—	—	—	—	—
26.2	424†	6.6	—	—	—	—	—	—
26.5	—	—	427	6	—	—	—	—
26.9	433	6	—	—	—	—	—	—
28.9	374†	4	—	—	—	—	—	—
33.0	—	—	315	5	—	—	—	—

*For the values of P_0 and t_i, see the corresponding run in Table 2.
†Hot channel, in which the instabilities occur first.
‡Location 225.

Table 2. Operating conditions for the unit

	Sodium side			Water/steam side			
Run No.	W (kg/s)	t_i (°C)	Q (MW)	W (kg/s)	t_i (°C)	t_0 (°C)	P_0 (MN/m^2)
1.3	170	452	21.2	13.0	286	394	16.7
2.4	170	442	18.9	11.5	286	396	16.7
2.5	170	442	18.1	10.7	286	409	17.0
3.7	174	421	14.8	8.6	286	395	17.0
4.4	179	403	8.7	4.7	286	400	16.7
13.2	174	440	18.1	11.5	302	404	16.7
13.4	173	443	15.1	9.2	301	418	16.6
14.0	183	440	22.3	13.9	260	364	16.8
14.2	182	442	20.0	10.8	260	410	16.7
14.3	186	442	19.5	10.0	260	419	16.7
14.4	186	441	18.1	9.2	259	418	16.5
14.5	179	441	16.1	8.7	259	414	16.8
15.0	172	439	21.8	12.8	240	374	16.8
15.4	173	441	18.8	9.8	240	416	16.7
19.7	122	408	10.4	6.2	300	337	12.8
19.8	121	408	10.1	5.5	300	359	12.2
20.3	125	411	12.5	7.4	280	330	12.3
21.3	123	408	12.2	6.8	260	330	12.3
21.8	120	412	10.5	5.7	260	356	13.4
22.1	124	409	11.9	6.5	240	337	13.4
26.2	126	434	12.1	6.7	301	422	16.2
26.5	126	436	12.9	7.4	301	418	16.3
26.9	127	441	14.5	8.4	300	411	16.2
28.9	121	386	11.3	5.9	281	324	9.2
33.0	62	351	6.6	2.5	214	305	5.3

operating conditions of the previous *stable* run were specified as the ICI for this tube (i.e. the temperature at the inlet of the tube and the temperature and pressure at the outlet of the tube). It was also checked whether the requirement is fulfilled that the temperature oscillations beyond the ICI reach a limit cycle and thereafter are sustained. The difference between the outlet temperature for the run specified as the ICI and the outlet temperature for the previous run did not exceed 10 K. During a run the total mass flow in the unit and the temperature and pressure at the outlet and inlet of the unit were kept constant.

For almost all test runs, instabilities were first detected in the tubes located at the outer tube bundle region; i.e. for the tubes numbered as 233 and 238 in Fig. 2. If the mass flow is decreased further, the tubes in the inner tube bundle region also become unstable. The operating conditions for the experiments are summarised in Tables 1 and 2.

Beyond the ICI, periodic outlet temperature oscillations were detected with amplitudes between 9 and 60 K and periods between 4 and 7.6 s. These periods suggest that the observed oscillations are of the density-wave type. An example of these oscillations is shown in Fig. 3.

During some runs, outlet temperature oscillations with small irregular periods and amplitudes of a few degrees Kelvin have also been observed. These instabilities will not be further considered since it is speculated that these are caused by multiple irregular interactions between flow rate, pressure drop and vapour generation rate due to mode of operation, viz.

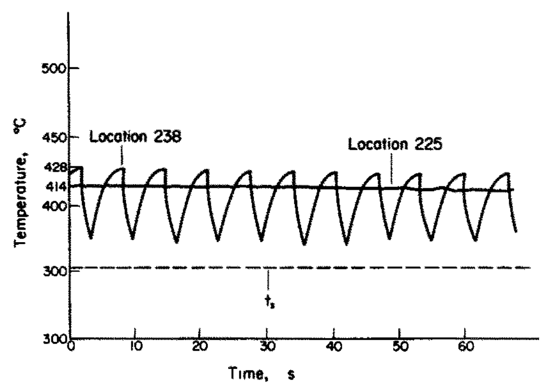

FIG. 3. Typical example of density-wave oscillations.

by decreasing the mass flow in the unit in small steps; these instabilities disappear after some minutes.

CORRELATION OF DATA

In general, to correlate the results of dynamic instability experiments, they are fitted into a theoretical stability model, which is a simultaneous solution of the three one-dimensional, non-steady state conservation equations (i.e. energy, momentum and mass) for the one-phase flow, subcooled boiling and boiling regions of a steam generator tube with appropriate boundary conditions [3–5, 7, 8, 12, 13, 15–17, 19, 24–26]. Since these three conservation equations include more than three unknowns for each of the flow regions mentioned above, subsidiary equations have to be used for reduction of the unknowns in the equations. These are correlations for the properties of water and steam, correlations for slip ratio, heat transfer and pressure drop for different flow regions of a steam generator tube, and a correlation for the thermodynamic non-equilibrium condition in the subcooled boiling- and superheated steam-region of a steam generator tube.

Three main approaches have been used in the literature for the solution of the three conservation equations: numerical or analog solution of the equations for given initial conditions and a given system (see for example [24]), linearisation and solution of the equations with the help of the feed-back theory (see for example [25]) and simplified analytical solution of the linearised equations (see for example [12, 26]). With the exception of the last approach, the use of a computer is in general necessary for the solution of the equations.

Almost every stability model presented in the literature assumes an axial uniform heat flux distribution, a condition which does not apply to the present experiments. Therefore the data presented in this study have been correlated with dimensional analysis.

Correlation of the ICI data

It was shown in [1] that in a steam generator tube across which pressure drop is constant, the enthalpy rise in the tube, or the steam quality at the outlet of the tube is constant for a given geometry, subcooling and pressure. The correlation given in [1] for the ICI excellently fits the present data but not the data of Quandt [13] obtained for a $0.00246 \times 0.0254 \times 0.686$ m electrically heated rectangular channel across which pressure drop was constant. Therefore the correlation given in [1] is modified to determine the outlet steam quality at the ICI:

$$(X_0)_I = 0.98\{0.038+0.0039 \times [\ln([1-P_r]P_r^{0.05})]^{-1}\} \times \left(\frac{L}{D}\right)^{0.51} (1+K)^{0.02} \times (1+1.7\exp[-50\Delta H_{sub}/H_s]). \quad (1)$$

At given operating conditions, instabilities will occur in the channel if the steam quality at the outlet of a boiling channel (evaluated by the use of equation (2)) exceeds the steam quality predicted by equation (1). Equation (1) fulfils the requirement that the steam quality is not defined at the critical pressure since $X = (H_0 - H_s)/r$ and $r = 0$ at the critical pressure. The steam qualities predicted by this equation are compared in Fig. 4 with the present data, the data given in [1] for a 10 m and an 18.84 m long sodium heated steam generator tube and the data of Quandt [13] for a 0.686 m long rectangular channel. The data are found to fit the equation well.

The following equations hold also for a boiling channel:

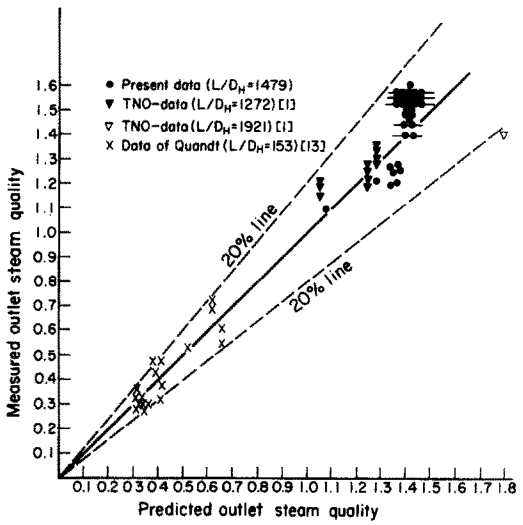

FIG. 4. Verification of equation (1).

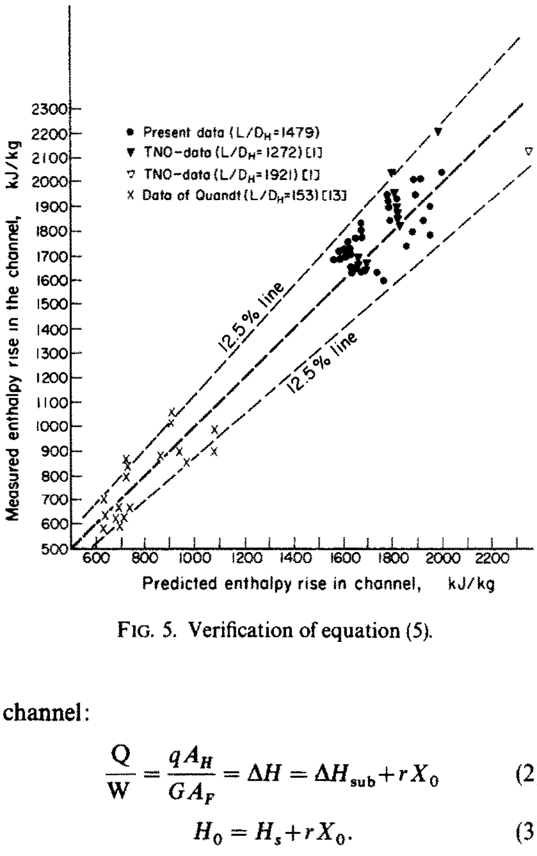

FIG. 5. Verification of equation (5).

$$\frac{Q}{W} = \frac{qA_H}{GA_F} = \Delta H = \Delta H_{sub} + rX_0 \quad (2)$$

$$H_0 = H_s + rX_0. \quad (3)$$

By inserting equation (1) into equation (2), the power or the enthalpy rise in a channel at the ICI can be predicted:

$$Q_I = W_I \Delta H_I = W_I\{(\Delta H_{sub})_I + (X_0)_I r\} \quad (4)$$

and

$$\Delta H_I = (\Delta H_{sub})_I + (X_0)_I r. \quad (5)$$

where $(X_0)_I$ in equations (4) and (5) is given by equation (1). Equation (5) is compared with the present data and the data of [1, 13] in Fig. 5, and it predicts very well the enthalpy rise in the test channels at the

ICI (or the *power* in the test channels at the ICI; compare equation (4) with equation (5)). The experimental ranges of the equations (1), (4) and (5) are:

$$\begin{aligned}(P_0)_I &= 4.1\text{–}17\,\text{MN/m}^2\\ (X_0)_I &= 0.27\text{–}1.59\\ (\Delta t_{sub})_I &= 3\text{–}111\,\text{K}\\ \Delta H_I &= 582\text{–}2130\,\text{kJ/kg}\\ L/D &= 153\text{–}1921\\ D_H &= 0.0045\text{–}0.0126\,\text{m}.\end{aligned}$$

In the present experiments, the heat flux (or power) and mass velocity were not measured in the tubes in which the instabilities were detected. The range of these operating conditions in the data given [1, 13] is: $G_I = 353\text{–}2088\,\text{kg/m}^2\,\text{s}$ and $(q_a)_I = 0.1\text{–}3.25\,\text{MW/m}^2$.

It follows from the equations (1) and (3) that the steam quality (or the enthalpy of the steam/water mixture or steam) at the outlet of a channel across which a constant pressure drop is maintained, is constant at the ICI for a given pressure, geometry and subcooling for low subcoolings ($[\Delta H_{sub}/H_s]_I < 0.1$) and for a given pressure and geometry at medium and high subcoolings. This is an *important result*. It can be used as a *boundary condition* additional to the boundary conditions used in the literature to solve the three conservation equations.

In accordance with equation (4), the other parameters being constant, the stability of a boiling channel may be increased by decreasing the heat flux, the heated length and the subcooling at low subcoolings and by increasing the mass velocity, the inlet pressure drop, the hydraulic diameter of the channel and the inlet subcooling at medium and high subcoolings. These results are in agreement with the experimental results of various investigators. Pressure can decrease or increase the degree of stability of a boiling channel, depending on its magnitude and on the subcooling, in accordance with equation (4). This result is not in agreement with that given in [15, 16] for a natural-circulation channel.

Equation (1) was compared with the ICI-data of Anderson (as quoted from [4]), Becker *et al.* [15], Levy and Beckjord [14], and Spigt [16] from natural circulation boiling systems. The aforesaid investigators used different types of short electrically heated test sections, i.e. annulus and tube, and the pressure in their experiments covered the range between 0.2 and 7 MN/m^2. The number of their ICI-data was 131. *As anticipated*, equation (1) did not fit these ICI-data, because the boundary condition used in the experiments of the aforesaid investigators, namely, a constant pressure drop across the whole loop, was different from the boundary condition used in the present experiments and those discussed in [1, 13], i.e. a constant pressure drop across a channel. Nevertheless for the natural circulation systems, it can also be shown by the use of the data of the aforesaid authors that the steam quality at the outlet of a channel or the enthalpy rise in a channel is constant at the ICI for a given geometry, subcooling, pressure and mass velocity.

Correlation of the period of the dynamic instabilities

A rather approximate correlation is found in the literature [8] indicating that the ratio of the period of the DWO to the transit time (of a fluid particle in a channel) varies between 1 and 2. This correlation will be verified below. In order to calculate the transit time, such factors as for instance the mass flow and the lengths of different flow regimes in a channel have to be known. In the present experiments these quantities were not measured. Therefore the transit time has been evaluated for the average operating conditions of the unit and is assumed to be equal to that in a tube for which the instabilities were detected. For the operating conditions of the present experiments, this assumption is not strict: If it is assumed that the same power is developed in every tube, then the average mass flow in the unit differs by at most 10% from that in a tube of the unit (see Tables 1–2 and $Q = W\Delta H$). A 10% variation in the mass flow can introduce only a few percent variation in the lengths of different flow regimes in a tube of the unit, since the pressure drop across the unit is constant. Furthermore, as will be seen later, a 10% error in the mass velocity is of second-order importance in correlating the data.

In order to determine the transit time in the unit, the data taken for the ICI-runs have been used and thermodynamic equilibrium in the boiling- and superheated steam region was assumed. The heat developed in the preheat region and that developed in the superheated steam region are then known. The lengths of these regions have been evaluated with the heat-exchanger formula:

$$Q = A_H U \Delta t_1 = 139\pi DLU\Delta t_1. \tag{6}$$

The length of the boiling region was determined by subtracting the sum of the lengths of the preheat- and superheated steam region from the effective tube length. The water/steam-side heat-transfer coefficient in the overall coefficient of heat transfer in equation (6) was evaluated with the well-known correlation of Dittus and Boelter as quoted from [27], and the sodium-side heat transfer coefficient in the overall coefficient of heat transfer in equation (6) with the correlation of Friedland *et al.* [28].

These heat-transfer coefficients were predicted at the arithmetic mean temperature and pressure both in the preheat- and superheated steam region. The properties of sodium, water and steam were taken from [29, 30]. The average density of the steam/water mixture in the boiling region was calculated from the equation below [1]:

$$(\rho_a)_b = \frac{\displaystyle\int_0^{L_b} \{(1-\alpha)\rho_s + \alpha\rho_v\}\,dz}{\displaystyle\int_0^{L_b} dz}. \tag{7}$$

The void fraction in equation (7) was evaluated with the correlation established by one of the authors [31]:

$$\beta/\alpha = 1 + \frac{0.36\,(1-P_r)^{0.9}\rho_v}{G\{X+(1-X)(\rho_v/\rho_s)\}} \tag{8}$$

where

$$\beta = \frac{X}{\{X+(1-X)(\rho_v/\rho_s)\}}. \quad (9)$$

The average density of the fluid in a single-phase flow region was predicted by using the arithmetic mean temperature and pressure in this region, and the transit time in the unit was calculated from the following formula [1]:

$$\xi = G_l^{-1}[L_p(\rho_a)_p + L_b(\rho_a)_b + L_S(\rho_a)_S]. \quad (10)$$

The present data and the data obtained from [1, 13] for the ratio of the period of the DWO to the transit time are plotted vs Froude number in Fig. 6. In [1] transit times are given. In order to calculate the transit times from the data of [13], equations (7) to (10) were used and thermodynamic equilibrium was assumed in the boiling region.

It follows from Fig. 6 that the above-mentioned ratio appears to be a function of the Froude number and can be as low as 0.25. Therefore the aforesaid correlation given in the literature for the period of the DWO is far from satisfactory.

In order to correlate the data, the following equation was used:

$$\frac{\zeta}{\xi_b} = Fr^{0.39}\left(0.9 - 0.6\frac{L_b}{L}\right) \quad (11)$$

where ξ_b, the transit time in the boiling region is

$$\xi_b = \frac{L_b(\rho_a)_b}{G_l}. \quad (12)$$

As shown in Fig. 7, equation (11) correlated the data of [1, 10] rather well and the present data well, thus permitting the assumption that the transit time in the unit is equal to that in a tube for which the instabilities were detected, and justifying the errors in predicting Fr and L_b. The experimental range of equation (11) is the same as that given for equation (1) and the measured periods varied between 0.35 and 7.6 s.

Evaluation of the hot-channel factor

A designer of a steam generator knows only the average operating conditions in the unit but not those in the hot channel where the instabilities occur first. In a steam generator there are many tubes, and operating conditions in every individual tube are different from the average operating conditions of the unit. Therefore, in order to apply equation (1) to a steam generator, a hot-channel factor has to be defined, which relates operating conditions in the hot-channel to those in the steam generator. Here the hot-channel factor will be defined as the ratio of exit steam quality in the hot channel to that of the unit. For the operating conditions considered in this study (see Tables 1 and 2), this ratio can be given by the correlation below:

$$\frac{(X_0)_l}{(X_0)_{sg}} = 0.616(2-P_r)\exp(2.2810^{-6}Re + 0.57\Delta H_{sub}/H_s) + 0.061 \quad (13)$$

for $Re \geqslant 3.51 \cdot 10^4$. The correlation is shown in Fig. 8.

In order to judge whether the instabilities occur in a steam generator for which the operating conditions are known, $(X_0)_l$ has first to be evaluated by using equation (1) and thereafter this $(X_0)_l$ has to be inserted into equation (13) to predict $(X_0)_{sg}$. If this $(X_0)_{sg}$ is lower than the steam quality at the outlet of the steam generator, the unit is susceptible to instabilities.

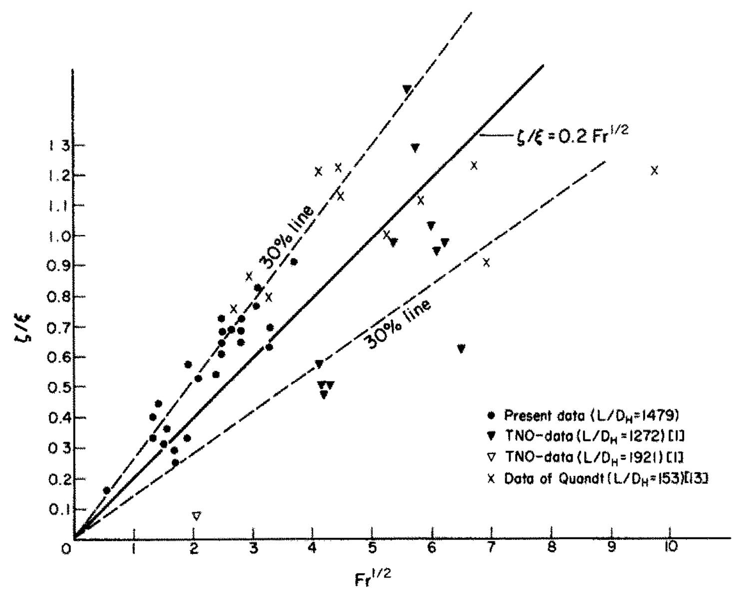

FIG. 6. Verification of the correlation from literature for the periods of the DWO.

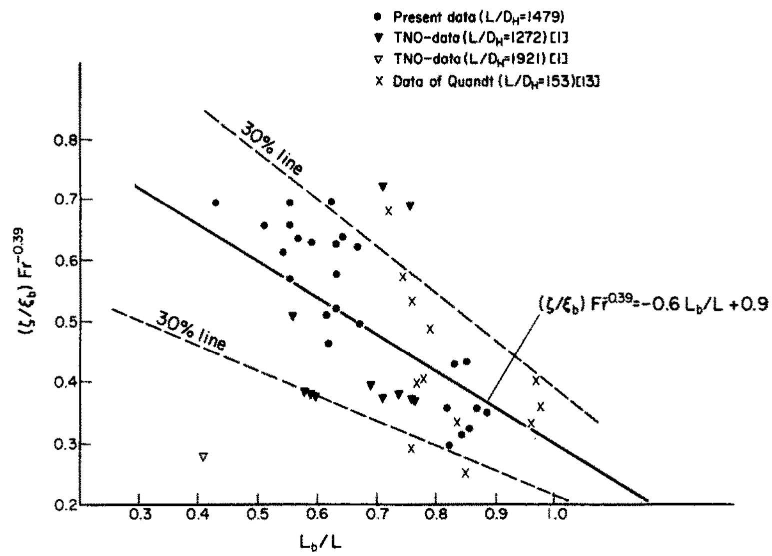

FIG. 7. Correlation of the data for the periods of the DWO.

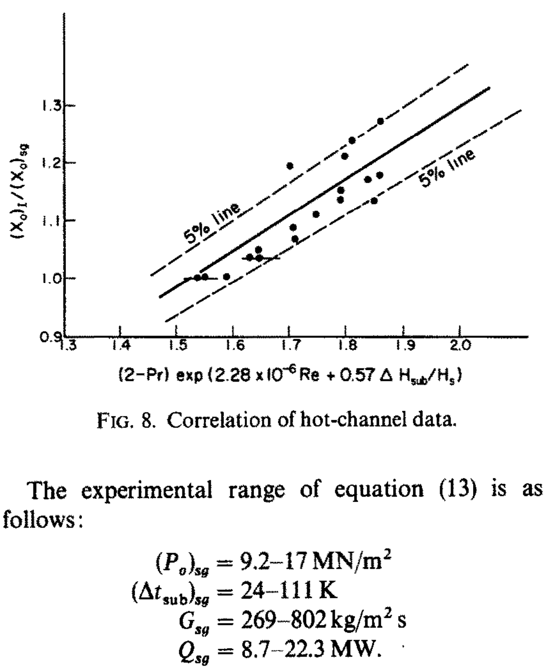

FIG. 8. Correlation of hot-channel data.

The experimental range of equation (13) is as follows:

$$(P_o)_{sg} = 9.2\text{–}17\,\mathrm{MN/m^2}$$
$$(\Delta t_{sub})_{sg} = 24\text{–}111\,\mathrm{K}$$
$$G_{sg} = 269\text{–}802\,\mathrm{kg/m^2\,s}$$
$$Q_{sg} = 8.7\text{–}22.3\,\mathrm{MW}.$$

CONCLUSION

Evidence is presented that the inception conditions and the periods of the so-called DWO can be predicted with simple equations for a wide range of operating conditions for a boiling channel across which the pressure drop is constant, thus eliminating the use of time-consuming complicated stability correlations in the form of a computer program. For most industrial applications, the prediction of the inception conditions and the periods of the DWO is sufficient.

Further experimentel and theoretical verification of the presented work is recommended, however.

Acknowledgement—This study is a government-sponsored work carried out at Neratoom and TNO. The authors wish to express their gratitude to Messrs. A. H. de Haas van Dorsser, K. A. Warschauer and C. Ch. Smit for their encouragement during the preparation of this work.

REFERENCES

1. H. C. Ünal, An investigation of the inception conditions of dynamic instabilities in sodium heated steam generator tubes. Paper presented at Nato Advanced Study Institute on Two-Phase Flows and Heat Transfer, Istanbul, Turkey (16–27 August 1976).
2. L. E. Efferding, DYNAM—a digital computer program for study of the dynamic stability of once-through boiling flow with steam superheat, GAMD-8656 (1968).
3. A. L. Davies and R. Potter, Hydraulic stability. An analysis of the causes of unstable flow in parallel channels, AEWW-R446 (1966).
4. L. G. Neal and S. M. Zivi, Hydrodynamic stability of natural circulation boiling systems, Vol. I, STL-372-14 (1) (1965).
5. T. Bjørlo, T. Eurola, R. Grumbach, P. Hansson, A. Olson, J. Rasmussen and K. Romslo, Comparative studies of mathematical hydrodynamic models applied to selected boiling channel experiments, in *Proceedings of the Symposium on Two-Phase Flow Dynamics*, EUR-4288e, Vol. 1, pp. 981–1057. Euratom, Brussels (1969).
6. T. Fallows, J. A. Hitchcock, R. C. Jones, J. Lis and E. W. Northover, A study of oscillatory instabilities in the parallel channels of a high pressure once-through boiler rig, in *Proceedings of the International Conference—Boiler Dynamics and Control in Nuclear Power Stations*, pp. 14.1–14.8. The British Nuclear Energy Society, London (1973).
7. *Proceedings of the Symposium on Two-Phase Flow Dynamics*, EUR-4288e, Vol. I and Vol. II. Euratom, Brussels (1969).
8. J. A. Bouré, A. E. Bergles and L. S. Tong, Review of two-phase flow instability, *Nucl. Engng Design* **25**, 165–192 (1973).
9. F. A. Jeclic and K. T. Yang, The incipience of flow oscillations in forced-flow subcooled boiling. NASA TM X-52081 (1965).
10. O. V. Remisov, V. A. Vorobyev, Yu. I. Gribanov and V. V. Sergeev, Statistical characteristics of temperature pulsations within post-burnout region, in *Proceedings of the Fifth International Heat Transfer Conference, Tokyo—*

1974, Vol. IV, pp. 215–219. J.S.M.E.–A.I.Ch.E., Tokyo (1974).
11. A. H. Stenning and T. N. Veziroglu, Flow oscillation modes in forced-convection boiling, in *Proceedings of the 1965 Heat Transfer and Fluid Mechanics Institute*, pp. 301–316. Stanford University Press, Palo Alto (1965).
12. J. A. Bouré, The oscillatory behaviour of heated channels—An analysis of the density effects—I. The Mechanism (non-linear analysis); II: The oscillations thresholds (linearised analysis), CEA R 3049 (1966).
13. E. R. Quandt, Analysis and measurements of flow oscillations, *Chem. Engng Prog. Symp. Ser.* **57**(32), 111–126 (1961).
14. S. Levy and E. S. Beckjord, Hydraulic instability in a natural circulation loop with net steam generation at 1000 psia, GEAP-3215 (1959).
15. K. M. Becker, S. Jahnberg, I. Haga, P. T. Hansson and R. P. Mathisen, Hydrodynamic instability and dynamic burnout in natural circulation two-phase flow. An experimental and theoretical study, AE-156 (1964).
16. C. L. Spigt, On the hydraulic characteristics of a boiling water channel with natural circulation, Ph.D. Thesis, Technical University of Eindhoven, The Netherlands (1966).
17. F. J. M. Dijkman, Some hydrodynamic aspects of a boiling water channel, Ph.D. Thesis, Technical University of Eindhoven, The Netherlands (1969).
18. J. D. Crowley, C. Deane and S. W. Gouse, Two-phase flow oscillations in vertical, parallel, heated channels, in *Proceedings of the Symposium on Two-Phase Flow Dynamics*, EUR-4288e, Vol. II, pp. 1131–1171. Euratom, Brussels (1969).
19. G. Yadigaroglu, A. E. Bergles, Fundamental and higher-mode density-wave oscillations in two-phase flow, *J. Heat Transfer* **94**, 189–195 (1972).
20. G. L. Wedekind and B. T. Beck, Correlation between outlet flowrate and mixture-vapor transition point oscillations in two-phase evaporating flow, in *Proceedings of the Fifth International Heat Transfer Conference, Tokyo*—1974, Vol. IV, pp. 220–224. J.S.M.E.–A.I.Ch.E., Tokyo (1974).
21. W. J. C. de Clercq and N. J. van Waveren, Steam-generator and intermediate heat-exchanger development, in *Sodium-Cooled Fast Reactor Engineering, Proceedings of a Symposium, Monaco, 23–27 March* 1970, pp. 433–451. IAEA, Vienna (1970).
22. P. W. P. H. Ludwig and B. M. Hus, Some results of the 50 MW straight tube steam generator test in the TNO 50 MW SCTF at Hengelo, Paper presented at IAEA Study Group Meeting on Steam Generators for LMFBR's, Bensberg (14–17 October 1974).
23. A. R. Braun, Sodium test facilities available at TNO, in *Proceedings of the Information Meeting—TNO Contribution to LMFBR Development, 10–11 May 1973, Utrecht, The Netherlands*, pp. 56–67. TNO, Apeldoorn (1973).
24. K. O. Solberg and P. Bakstad, A model for the dynamics of nuclear reactors with boiling coolant with a new approach to the vapour generation process, in *Proceedings of the Symposium on Two-Phase Flow Dynamics*, EUR-4288e, Vol. I, pp. 871–933. Euratom, Brussels (1969).
25. A. B. Jones, Hydrodynamic stability of a boiling channel, KAPL-2170 (1961).
26. N. Zuber, Flow excursions and oscillations in boiling, two-phase flow systems with heat addition, in *Proceedings of the Symposium on Two-Phase Flow Dynamics*, EUR-4288e, Vol. I, pp. 1071–1089. Euratom, Brussels (1969).
27. J. G. Knudsen and D. L. Katz, *Fluid Dynamics and Heat Transfer*, p. 394. McGraw-Hill, New York (1958).
28. A. J. Friedland, O. E. Dwyer, M. W. Maresca and C. F. Bonilla, Heat transfer to mercury in parallel flow through bundles of circular rods, in *Proceedings of the 1961 International Heat Transfer Conference, Boulder, Colo., 28 August–1 September*, 1961, Vol. III, paper 62. ASME, New York (1961).
29. M. E. Durham, The thermodynamic and transport properties of liquid sodium, CEGB Report RD/B/M2479 (Revised)-CFR/THWP/P(72) 28 (Revised) (1974).
30. The American Society of Mechanical Engineers, 1967 *ASME Steam Tables*. ASME, New York (1967).
31. H. C. Ünal, Void fraction and incipient point of boiling during the subcooled nucleate flow boiling of water, *Int. J. Heat Mass Transfer* **20**, 409–419 (1977).

LES INSTABILITES DYNAMIQUES DANS LES CANAUX D'UNE CHAUDIERE A VAPEUR A HAUTE CAPACITE, CHAUFFEE AU MOYEN DE SODIUM

Résumé—On a observé des instabilités dynamiques d'un type de densité oscillatoire dans les canaux d'une chaudière à vapeur à haute capacité chauffée au moyen de sodium. Les amplitudes maximales de ces oscillations varient entre 9 et 60 K et les périodes entre 4 et 7,6 s.

Nos données expérimentales pour les périodes et les conditions de début des instabilités dynamiques, ainsi que les données trouvées dans la littérature pour un canal circulaire et un canal rectangulaire avec une chute de pression constante ont été corrélées à l'aide de simples équations pour la gamme des conditions suivantes: pression 4,1–17 MN/m^2; qualité de vapeur à la sortie des canaux 0,27–1,59; sous-refroidissement à l'entrée des canaux 3–111 K; rapport de la longueur chauffante au diamètre hydraulique: 153–1921; diamètre hydraulique 0,0045–0,0126 m; augmentation de l'enthalpie dans le canal: 582–2130 kJ/kg; vitesse massique 353–1088 kg/m^2 s; flux de chaleur moyen: 0,1–3,25 MW/m^2; période des oscillations 0,35–7,6 s.

Au début des instabilités dynamiques, le qualité de vapeur (ou l'enthalpie de la vapeur ou du mélange d'eau et de vapeur) à la sortie d'un canal bouillant est constante pour un certain refroidissement, une certaine pression et une géométrie dans la gamme des faibles refroidissements, et pour une certaine pression et une géométrie dans la gamme des refroidissements intermédiaires et elevés.

La période des instabilités dynamiques est fonction du temps de résidence d'une particule fluide dans la région bouillante d'un canal, du nombre de Froude et du rapport de la longueur de la région bouillante à la longueur totale chauffée.

Un facteur relatif au canal chauffant a été également établi, qui relie les conditions d'opération dans le canal pour lequel les instabilités dynamiques se présentent la première fois, aux conditions moyennes d'opération dans le générateur de vapeur.

DYNAMISCHE INSTABILITÄTEN IN ROHREN EINES NATRIUMBEHEIZTEN GERADROHR-ZWANGSDURCHLAUF-DAMPFERZEUGERS GROSSER LEISTUNG

Zusammenfassung—In den Rohren eines natriumbeheizten Dampferzeugers mit großer Leistung werden dynamische Instabilitäten vom Typ "density wave" beobachtet. Die Amplituden von Extremwert zu Extremwert dieser Schwingungen variierten zwischen 9 und 60 K, und die Perioden variierten zwischen 4 und 7,6 s. Unsere experimentellen Daten für die Perioden und die Entstehungsbetriebszustände sowie die in der Literatur für ein Rohr und einen rechteckigen Kanal mit konstantem Druckverlust gefundenen Daten sind mit einfachen Gleichungen für die nachstehenden Betriebsbereiche korreliert worden:

Druck	4,1–17 MN/m^2
Dampfgehalt am Austritt	0,27–1,59
Unterkühlung am Eintritt	3–111 K
Verhältnis beheizter Länge zum hydraulischen Durchmesser	153–1921
hydraulischer Durchmesser	0,045–0,0126 m
Enthalpiezunahme im Kanal	582–2130 kJ/kg
Massenstromdichte	353–2088 kg/m^2 s
mittlere Wärmestromdichte	0,1–3,25 MW/m^2
Periode	0,35–7,6 s.

Bei Beginn der dynamischen Instabilitäten ist der Dampfgehalt (oder die Enthalpie des Dampfes oder des Dampf/Wasser-Gemisches) am Austritt eines Dampfkanals im Falle einer gegebenen Unterkühlung, eines gegebenen Druckes und einer gegebenen Geometrie im Bereich der niedrigen Unterkühlungen und für einen gegebenen Druck und eine gegebene Geometrie für den Bereich der mittleren und größeren Unterkühlungen konstant. Die Periode der dynamischen Instabilitäten ist eine Funktion der Durchströmungszeit eines Teilchens im Siedebereich eines Kanals, der Froude-Zahl und des Verhältnisses der Siedebereichslänge zur gesamten beheizten Länge. Ein Heißkanal-Faktor, der die Betriebszustände in dem Rohr, worin die dynamischen Instabilitäten zuerst auftreten, mit den mittleren Betriebszuständen im Dampferzeuger in Beziehung setzt, ist auch erstellt worden.

ДИНАМИЧЕСКАЯ НЕУСТОЙЧИВОСТЬ В ТРУБАХ ПРЯМОТОЧНОГО ПАРОГЕНЕРАТОРА БОЛЬШОЙ ПРОИЗВОДИТЕЛЬНОСТИ, РАБОТАЮЩЕГО НА НАТРИИ

Аннотация — В трубах парогенератора большой производительности, работающего на натрии, обнаружено наличие динамической неустойчивости типа волн плотности. Колебания амплитуды составляли 9–60 K период 4–7.6 сек.

Наши экспериментальные данные по периодам и условиям возникновения динамических колебаний, а также опубликованные данные для трубы и прямоугольного канала с постоянным перепадом давления описывались простыми уравнениями для следующих условий: давление: 4,1–17 Мн/м^2; характеристики на выходе: 0,27–1,59; недогрев на входе: 3–111 K; отношение нагретой длины к гидравлическому диаметру: 153–1921; гидравлический диаметр: 0,0045–0,0126 м; прирост энтальпии в канале: 582–2130 к Дж/кг; массовый расход: 353–2088 кг/м^2 сек.; средний тепловой поток 0,1–3,25 Мвт/м^2; период: 0,35–7,6 сек. При возникновении динамической неустойчивости истинное паросодержание (энтальпии пара или пароводяной смеси) на выходе из канала с кипящей жидкостью является величиной постоянной при заданных значениях недогрева, давления и геометрии канала в диапазоне незначительного недогрева и при заданном давлении и геометрии в диапазонах среднего и значительного недогрева.

Период колебаний является функцией времени прохождения элемента жидкости в кипящей зоне канала, числа Фруда и отношения длины кипящей зоны к общей длине нагретого канала. Также получен коэффициент для горячего канала, соотносящий рабочие условия в трубе, в которой возникает динамическая неустойчивость, со средними рабочими условиями в парогенераторе.